**Preprints of the 7th IFAC Symposium on
Fault Detection, Supervision and Safety of Technical Processes
Barcelona, Spain, June 30 - July 3, 2009**

KV_C007
Villez, K., Keser, B., Rieger, L. (2009). Qualitative Representation of Trends (QRT) as a tool for automated data-driven diagnostics for on-line sensors. Proceedings of the 7th IFAC Symposium on Fault Detection, Supervision and Safety of Technical Processes (SafeProcess2009), Barcelona, Spain, 30 June-July 3, 2009, 1276-1281.

Qualitative representation of trends (QRT) as a tool for automated data-driven monitoring of on-line sensors

Kris Villez*,. Benjamin Keser*, Leiv Rieger***

** modelEAU, Université Laval, Pavillon Pouliot, 1065 av. de la Médecine, Quebec G1V 0A6, Canada*

*** Laboratory of Intelligent Process Systems (LIPS), Purdue University, Forney Hall of Chemical Engineering, 480 Stadium Mall Drive, West Lafayette, IN 47906, USA*

e-mail: kris.villez@gmail.com, benjamin.keser@uni-due.de, leiv.rieger@gci.ulaval.ca

Abstract: The application of on-line sensors for monitoring or real-time control of wastewater treatment plants remains a challenging problem. The primary cause for this is the unknown quality of the data obtained by such on-line instruments. In the presented work sensor-internal meta-data is used for self-diagnosis. It is verified whether the complete measurement profiles obtained during regular measurement cycles of a phosphate analyzer can help to assess the sensor's status and even indicate potential faults causing faulty behaviour. A qualitative analysis approach is taken and the obtained results indicate that measurement profiles are indeed affected by the implied fault scenarios and may thus serve for proper fault detection and diagnosis.

1. INTRODUCTION

In the last decades, a diverse set of control strategies of biological systems such as wastewater treatment plants has been developed in view of cost-effectiveness and increased treatment performance (Olsson *et al.*, 2005). However, advanced nutrient control strategies remain hardly implemented for full-scale systems. Barriers to overcome are the unknown and sometimes poor quality of on-line sensor data and the limited flexibility of the given control algorithms when faced with sensor failures. The first and most serious problem is dealt with in this article.

State of the art in monitoring on-line sensors is to compare reference measurements with the sensor values (e.g. Thomann *et al.*, 2001). More advanced strategies use statistical methods to detect faults from the measured time series (Rosén *et al.,* 2003). All these methods are based on the measurements itself. The strategy used in this work is to use available information contained inside the sensor (referred to as meta-data as in Rieger and Vanrolleghem, 2008) to check the sensor's functioning and behaviour. In the presented case, phosphate concentrations are measured by means of light intensity measurements before and after a colour reaction. The potential of using the light intensity measurements measured at other times during the measuring cycles is evaluated in this paper.

Given previous successes for data analysis with respect to a batch process for nutrient removal (Villez *et al.*, 2008), qualitative representation of trends (QRT) was chosen as the formal framework to analyze the available time series (Cheung and Stephanopoulos, 1990). QRT uses qualitative indicators such as 'steady-state', 'upward trend' and 'downward trend' to describe time series. The method by Bakshi and Stephanopoulos (1994) is used for this purpose, incorporating improvements for detection of consecutive inflection points (Villez, 2007; Villez *et al.*, submitted). This extended method is combined with the wavelet-based method for steady state identification (SSID) by Cao and Rhinehart (1995) to enable the identification of steady state episodes. For an overview of wavelet-based tools in signal processing the reader is referred to Ganesan *et al.* (2004). Alternative methods can be found in Flehmig *et al.* (1998), Akbaryan and Bishnoi (2000), Charbonnier *et al.* (2005), Dash *et al.* (2004), Rengaswamy and Venkatasubramanian (1995) and Wang and Li (1999). Qualitative representation of trends is typically aimed at process diagnosis, see e.g. in Akbaryan and Bishnoi (2001) and Rubio *et al.* (2004), or process data mining as in Stephanopoulos *et al.* (1997).

This contribution continues as follows. First, in Material and Methods, the experimental setup and the deployed technique for qualitative analysis are given. Secondly, the results are presented and discussed in Results and Discussion. Thirdly and lastly, conclusions and perspectives are provided.

2. MATERIALS AND METHODS

2.1 Sensor setup and operation

A Stamolys-CA71PH sensor from Endress+Hauser, Germany with a measuring range of 0.05 to 2.50 PO_4-P mg/l is used in this study. Its measuring principle is based on the automated ascorbic acid reduction method (APHA *et al.*, 2005). A scheme of the analyzer is shown in Figure

1. Throughout the measuring cycle which lasts 10 minutes, light is sent through the measurement cell. Each second, the light intensity leaving the measurement cell is measured as the frequency of electrons moved within the photo-electric sensor. Figure 2a shows profiles of this frequency measurement along typical measuring cycles.

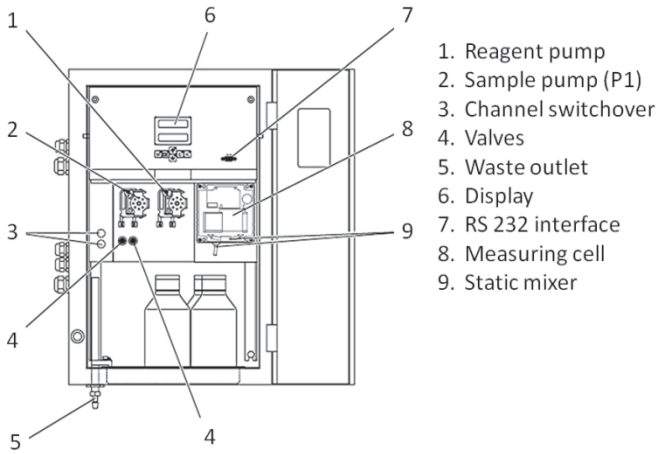

Figure 1. Scheme of the Stamolys-CA71PH phosphates analyzer

A single measurement cycle proceeds as follows (see Figure 2a). The measurement cell is flushed with sample solution in the phase 1 (P1). Five consecutive reference frequency measurements are taken in the phase 2 (P2). In the third phase (P3). The mixture of two reactive solutions, denoted A and B, is added to the measurement cell in phase 3 (P3). The initiated reaction continues in phase 4 (P4). After a fixed reaction time of 6 minutes, 5 consecutive frequency measurements are taken (phase 5, P5). In phase 6 (P6), the measurement cell is flushed with fresh sample to prepare the sensor for the next measuring cycle. The difference between the means of the consecutive frequency measurements taken in phase 5 and in phase 2 is computed at the end of phase 5. The sensor measurement is then obtained by means of a linear calibration curve between the phosphate concentration and this difference. Standard use of the sensor assumes that the measured frequency does not change in phase 2 and 5, i.e. that steady-state is achieved.

2.2 Fault experiments

Several faults were inflicted onto the sensor while operating. The fault scenarios were selected on the basis of their foreseen effects on the frequency measurements and relate essentially to the missing of one or more of the reactive components in the measurement cell, e.g. sample or reagents. A set of normal measuring cycles, i.e. without faults, were retained for analysis as well. This set of normal cycles is split into normal cycles with and without phosphate in the sample. The latter were specifically set up for comparison with sensor response in the absence of solution. For the pump failure experiment, the first cycle was run normal and the pump was put off right before the beginning of the second cycle. Table 1 presents the discerned conditions of the sensor and the corresponding descriptions and numbers of measuring cycles. Artificial sample solutions were used with concentrations of 0.00, 1.02, 1.55, 1.59 and 2.05 PO_4^--P mg/l.

Table 1. Tested conditions of the sensor, description of conditions and number of cycles in each condition

Condition	Description	#
N1: normal non-zero	No faults and at detectable phosphate concentrations	4
N0: normal zero	No faults, zero phosphate concentrations	3
F1: no sample	The sample container is empty	3
F2: blocked sample tube	No new sample can enter the vial	7
F3: blocked reagent A tube	No new reagent A can enter the measurement vial	5
F4: blocked reagent B tube	No new reagent B can enter the vial	4
F5: pump failure	The reagent pump fails to work	2

2.3 Method 1: Qualitative Representation of Trends (QRT)

The framework by Cheung and Stephanopoulos (1990) for a qualitative description of trends is based on the signs of the first and second derivatives of a signal. Both are classified as zero, positive or negative and according to these classes 7 qualitative descriptors, also called triangular primitives, are defined and tagged with a unique character. Table 2 summarizes this alphabet.

Given the triangular primitives, a qualitative description of a time series consists of a set of contiguous episodes for which the start time, end time and the triangular primitive is assessed. A wavelet-based method for Qualitative Representation of Trends (QRT) is used for identification of the qualitative description (Bakshi and Stephanopoulos, 1994; Villez, 2007; Villez *et al.*, submitted). In the presented case, the included wavelet scales range from 1 to 7 (wavelet support ranging from 2 to 2^7=128 samples).

Table 2. Signs of derivatives and corresponding character for the triangular primitives

Derivatives		Triangular primitive
1st	2nd	
+	−	A
−	−	B
−	+	C
+	+	D
+	0	E
−	0	F
0	0	G

Despite the formal definition of the triangular primitive *G* for steady state behaviour, the latter method generally does not deliver this description for noisy steady-state sequences (Villez, 2007). However, steady state is of importance for the studied analyzer given that steady behaviour is assumed in P2 and P5 of the measuring cycle and is a prerequisite for a proper phosphate measurement.

2.4 Method 2: Steady-State Identification (SSID)

The steady-state identification (SSID) method by Cao and Rhinehart (1995) was adopted for detection of steady-state behaviour. This method uses three exponential filters with respective parameters λ_1, λ_2 and λ_3. The first filter is used for the time series itself:

$$x_f(k) = (1 - \lambda_1)\, x_f(k-1) + \lambda_1\, x(k) \quad (1)$$

with x(k): the raw signal at time instant k

$x_f(k)$: the filtered signal a time instant k

The second filter provides an adaptive estimate for the variance of the filtered time series as follows:

$$v_f^2(k) = (1 - \lambda_2)\, v_f^2(k-1) + \lambda_2 \left(x(k) - x_f(k-1)\right) \quad (2)$$

with $v_f^2(k)$: the variance estimate at time instant k

A variance estimate for the original signal is found as follows:

$$\delta_f^2(k) = (1 - \lambda_3)\ \delta_f^2(k-1) + \lambda_3 \left(x(k) - x(k-1)\right)^2 \quad (3)$$

with $\delta_f^2(k)$: the variance estimate at time instant k

Now, the following test statistic is constructed:

$$R(k) = \frac{(2-\lambda_1)\, v_f^2(k)}{\delta_f^2(k)} \quad (4)$$

Cao and Rhinehart (1997) provide the confidence limits for this statistic under the null hypothesis of steady state for different settings of these forgetting factors. In this study, the filter parameters (λ_1, λ_2 and λ_3) were set to 0.5, 0.1 and 0.1 and the corresponding 99%-confidence limit was applied for steady-state testing.

2.5 Combined method

To enhance the existing QRT method so that steady periods are identified, steady-state behaviour, *G*, is accepted if the SSID method indicates steady-state for 10 or more consecutive samples. If not, the qualitative description by the wavelet-based method is accepted.

3. RESULTS AND DISCUSSION

3.1 Normal cycles with non-zero concentration (N1)

Figure 2a shows the light intensity profiles for the four fault-free cycles with non-zero phosphate concentrations in chronological order (1&2: 1.59 mg/l; 3: 1.02 mg/l, 4: 2.05 mg/l). In Figure 2b the measurements are rescaled by adding a separate offset for each cycle so that the profiles are separated from each other. The same will be done in following (Figures 3 to 6). The fault-free profiles are characterized by a steady behaviour at the beginning of the measurement cycle followed by a descent due to the colour reaction after addition of the reagents. As the vial is purged, the light intensity rises again to a level close to its initial level, as is typical for the device. The respective measurement results given by sensor output reading (for profile 1 to 4) were 1.75, 1.59, 1.05 and 2.16 mg P/l, thus delivering measurement errors ranging between 0.00 and 0.16 mg P/l.

Figure 2c shows the qualitative representations of the same time series. For all series, an initial steady section is indicated, *G*, after which a *BC* sequence expresses the downward trend observed earlier (first decelerating then accelerating). The results for the first and third series are characterized by a *DAG* sequence (upward trend, first accelerating then decelerating, and steady trend) after this BC sequence. The 2nd series exhibits a DG sequence only. Visual inspection of the first 3 series confirms that the signal rises, even though to minimal extent, after the *BC* sequence. This is not observed for the 4th series as a steady trend, *G*, follows directly after the *BC* sequence. Also, one notices that the *C* episode is longer than for the first 3 series. Also, inspection of Figure 2a confirms that steady state is reached later. This is attributed to a higher phosphate concentration (2.05 mg/l) incurring a longer reaction time compared to the other samples. After the second *G* episode, a *DA* sequence follows shortly after the start of purging of the measurement vial in all cycles. It is noted that the *D* episode is very short which indicates that the maximal speed of the light intensity rise is reached fast. In summary, the qualitative representations of the studied normal signals are found consistent with the behaviour of the actual data.

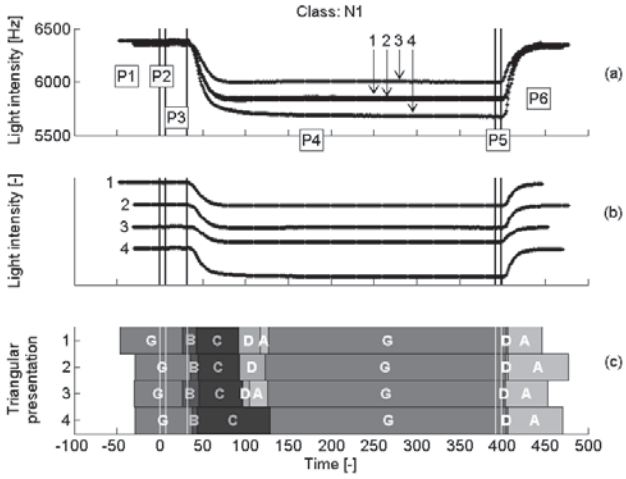

Figure 2. (a) Original and (b) rescaled measurement profiles and (c) qualitative analysis results for the normal cycles with non-zero phosphate concentrations (1&2: 1.59 mg/l; 3: 1.02 mg/l, 4: 2.05 mg/l). Vertical lines indicate the start and end of the discerned phases, tagged P1 to P6.

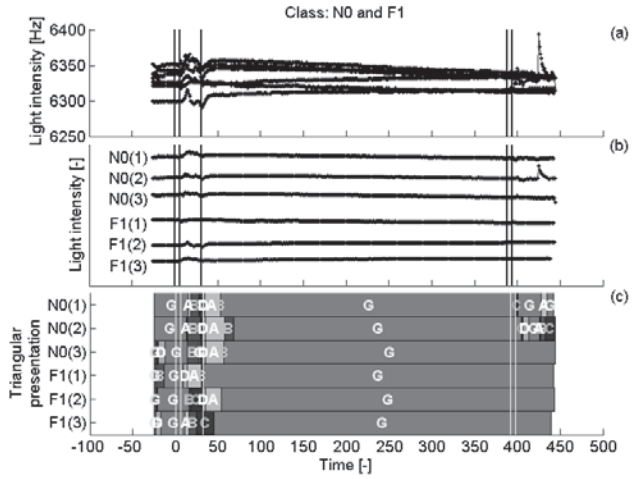

Figure 3. (a) Original and (b) rescaled measurement profiles and (c) qualitative analysis results for the normal cycles with zero phosphate concentrations (N0) and the abnormal cycle where no sample is present (F1). Vertical lines indicate the start and end of the phases of the measuring cycle.

3.2 Normal cycles with zero concentration (N0) and abnormal cycles corresponding to the absence of sample solution (F1)

In Figure 3, results obtained for the normal cycles with zero phosphate concentration (N0(1..3)) and the abnormal cycles without sample (F1(1..3)) are shown together. From Figure 3a and 3b, it is difficult, if not impossible, to differentiate the two conditions from each other. All cycles show steady behaviour over the whole cycle except during the period where chemicals are added to the measurement cell (P3). The N0(2) profile exhibits an unexplained rise of the signal followed by a slower return to its previous level.

The qualitative analysis results (Figure 3c) confirm the observations made in the previous paragraph. Indeed, the series are annotated as *G* over the major part of their lengths. Non-steady primitives are assigned in the periods preceding the reaction period and at the beginning of the reaction period. In addition, dynamic behaviour is indicated at the end of the N0(1) and N0(2) profiles. This is due to noise in the first case and due to the described jump event in the second case. With the exception of the latter two cycles, steady behaviour is indicated at the end of the cycles, contrasting with the normal cycles where flushing causes an upswing of the light intensity (Figure 2).

3.3 Cycles with blocked sample tube (F2)

Figure 4 shows the results obtained for the applied interruption of the sample feed (F2). The displayed measuring cycles were performed consecutively using a phosphate standard of 1.02 mg P/l. It can be seen in Figure 4a that during the first profile the reaction seems to proceed as normal. Indeed, a rather steady behaviour is followed by a downward trend which levels off by the end of the reaction period. In contrast to the normal cycles though, the light intensity does no return to its initial level. This can be expected as no fresh sample is added to the measurement cell. During the following cycles, the overall net change in light intensity becomes smaller, which is equally due to the absence of new reactive compounds. Even more, in the flushing phase of cycles 4 to 7, no visually detectable change in light intensity occurs anymore. At the beginning of the cycle, during the phase preceding the reaction period, and contrasting with the behaviour throughout the other periods of the measuring cycles, fluctuations of the light intensity occur due to addition of fresh chemical reagents (P2). The respective measurements given by sensor display reading were 0.75 mg P/l for the first cycle and 0.00 mg P/l for every following measurement. So, by the second faulty cycle, the sensor shows no response anymore to the phosphate concentration.

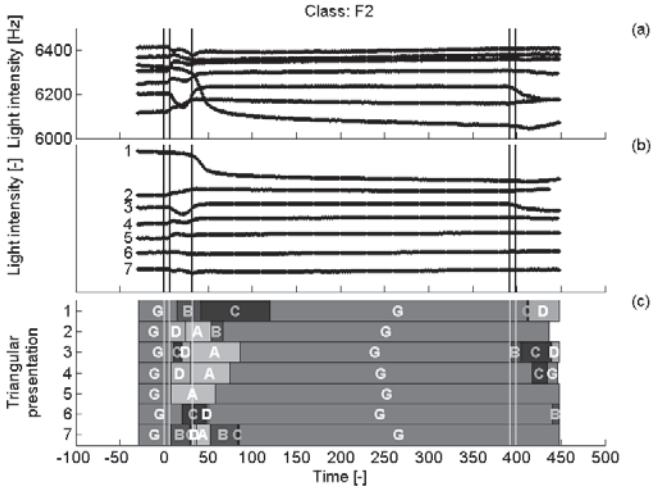

Figure 4. (a) Original and (b) rescaled measurement profiles and (c) qualitative analysis results for the cycles with blocked sample tube (F2). Vertical lines indicate the start and end of the phases of the measuring cycle. All cycles are performed with a 1.02 mg P/l standard solution.

The findings above are largely confirmed by QRT. The qualitative labelling of the first cycle, *GBCGCD,* matches indeed very well with the earlier description. The same is true for the other cycles except for cycles 3 to 5. Indeed, visual inspection confirms the upward trend, *A*, but also adds a descent, *BC*, before the steady period, *G*. The magnitude of this descent is too small to be detected in the qualitative analysis. Notable is the steady behaviour in P6 in cycles 5 to 7 and the upward trends indicated in the period before and during the reaction period (cycles 2 to 5).

3.3 Cycles with plugged reagent A tube (F3)

In Figure 5, results obtained for fault condition F3, absence of reagent A, are shown. All measuring cycles were performed consecutively using a phosphate standard of 2.05 mg P/l. It can be observed that the first cycle behaves similar to a fault-free cycle (Figure 1a). This indicates that the reagent tubes still contained enough of the solution to enable a normal reaction. In the following cycles, the most notable difference is the later occurrence of the downward trend during the reaction time. In addition, the 4th profile is characterized by an upswing of the light intensity during the reaction time before the largest downward trend is observed.

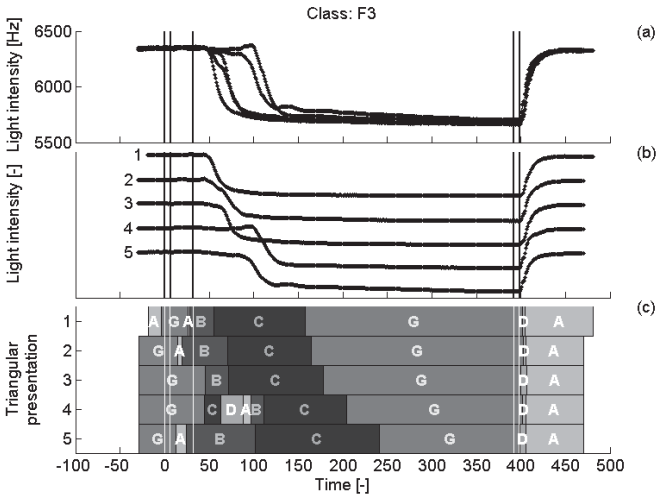

Figure 5. (a) Original and (b) rescaled measurement profiles and (c) qualitative analysis results for the cycles with blocked reagent A tube (F3). Vertical lines indicate the start and end of the phases of the measuring cycle.

These results are confirmed by qualitative analysis (Figure 5c). While the downward trend is still starting with the reaction time, the point of maximal (absolute) speed during the downward trend is clearly delayed. The *BC* transition occurs at 55 seconds for the first cycle, at about 70 seconds for cycles 2 and 3 and at about 105 seconds for cycles 4 and 5. The time at which the second *G* episode starts gradually evolves from 158 seconds for the first measuring cycle to 241 seconds in the 5th cycle. The respective measurements were 2.16, 2.17, 2.19, 2.11 and 2.06 mg P/l. In this case, the fault has thus a limited effect, at least in the first cycles, on the sensor performance (measurement errors between -0.14 and -0.01 mg P/l).

3.4 Cycles with plugged reagent B tube (F4)

Figure 6 provides the results for the measuring cycles operated under absence of reagent B (F4), also measured consecutively using a phosphate standard of 1.55 mg P/l. Similar to the previous case, it can be seen that the behaviour in the first cycle is largely unaffected (Figure 6a, 6b). Enough solution of reagent B is thus still available in the respective tubes. The effects on the next cycles are however more dramatic than for the F3 case. No steady behaviour is reached during P4 of the second cycle. Almost no reactivity is observed as from the third cycle, resulting in a minimal change of light intensity over the reaction phase. QRT results indicate the observed anomalies as well. For example, the inflection point in the *BC* sequence is already at approximately 150 seconds. Small oscillations in P4 for profile 3 result in a more complex description from the QRT method. Measuring cycle 4 is not affected by such oscillations and thereby the measurement is assessed to be in steady state over the whole length of the profile. The respective sensor readings were 1.58, 1.05, 0.31 and 0.00 mg P/l, which reflect1 the gradual change in sensor response to the phosphate compound.

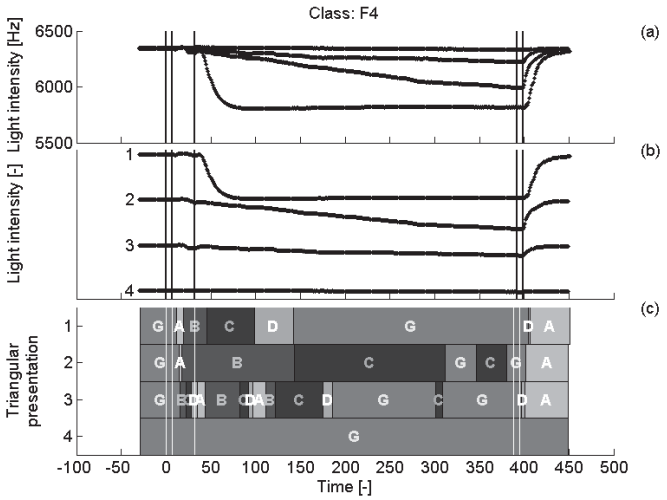

Figure 6. (a) Original and (b) rescaled measurement profiles and (c) qualitative analysis results for the cycles with blocked reagent B tube (F4, 1.55 mg P/l). Vertical lines indicate the start and end of the phases of the measuring cycle.

3.4 Cycles corresponding to the reagent pump failure (F5)

Figure 7 shows results for the two consecutive cycles exhibiting a failure of the pump for reagent B throughout the second cycle (1.02 mg P/l). The first cycle thus behaves normally and so is confirmed by qualitative analysis. In the second cycle, a flat curve is observed, indicating that no reaction has occurred. Qualitative analysis results confirm this, despite the inclusion of small oscillations in the qualitative analysis result of the second cycle.

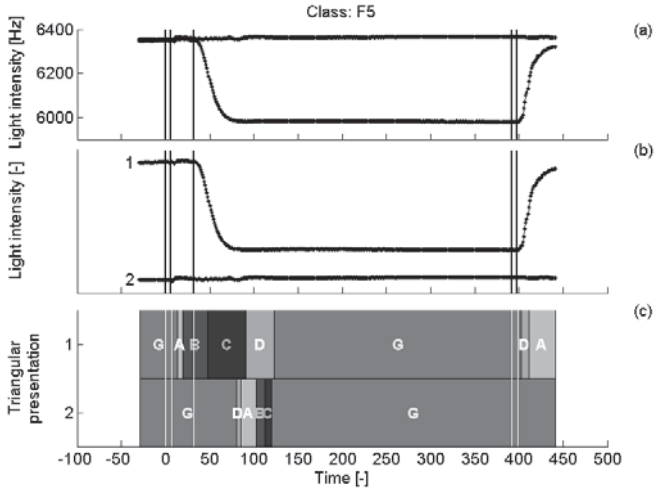

Figure 7. (a) Original and (b) rescaled measurement profiles and (c) qualitative analysis results for the pump failure experiment (F5, 1.02 mg P/l). Vertical lines indicate the start and end of the phases of the measuring cycle.

3.6 Summary and discussion

It is observed that the obtained qualitative descriptions match the results of visual inspection well and that the QRT result is affected in all fault scenarios. Indeed, for all faults considered, the light intensity measurement profile changes in the first or second cycle after the start of the fault, except for fault F3 (no

reagent A). Moreover, the inflicted faults simultaneously lead to serious measurement errors shortly after start of the fault, except for fault F3. As such, the qualitative analysis is considered useful as an indicator of sensor performance. The QRT is therefore promising for automated monitoring, i.e. fault detection, tasks and will be included in the fault detection scheme that is under development in our study.

Except when reagent A is absent, all the faults lead eventually to the observation of a rather flat profile since no reaction occurs due to the missing of reagent B or fresh sample. This truly anomalous behaviour is however hard to separate from the normal behaviour during cycles with zero phosphate concentration. While the qualitative analysis provides fault detection, we consider diagnosis impossible without further development or additional information.

5. CONCLUSIONS AND PERSPECTIVES

In this contribution, the use of light intensity measurements of a complete reaction cycle for sensor monitoring and diagnostics has been investigated. It has been shown that the studied profiles change qualitatively due to the studied faults and have potential for the automation of monitoring, i.e. fault detection tasks.

It has also been shown that qualitative analysis may provide a promising track for automation of fault detection and diagnosis tasks. Indeed, the observed faulty profiles change eventually to a flat profile for the following cases: blocking of the sample tube, absence of sample or reagent B and failure of the reagent pump. For absence of reagent A, a delay in the observed qualitative descriptions is observed.

It is therefore concluded that the use of internal meta-data analysed by the proposed extended QRT method allows automatic detection of sensor faults. Still, flat profiles resulting from a zero phosphate concentration are difficult to separate from the truly anomalous profiles. In view of solving this problem and in view of diagnosis, the inclusion of historical or additional information is suggested.

REFERENCES

Akbaryan, F. and P.R. Bishnoi (2000). Smooth representation of trends by a wavelet-based technique. *Comput. Chem. Eng,.* **24,** 1913-1943.

Akbaryan, F. and P.R. Bishnoi (2001). Fault diagnosis of multivariate systems using pattern recognition and multisensor data analysis technique. *Comput. Chem. Eng.,* **25,** 1313-1339.

Bakshi, B. and G. Stephanopoulos (1994). Representation of process trends - Part III. Multiscale extraction of trends from process data. *Comput. Chem. Eng.,* **18,** 267-302.

Cao, S. and R.R. Rhinehart (1995). An efficient method for on-line identification of steady state. *J. Process Control,* **5,** 363-374.

Cao, S. and R.R. Rhinehart (1997). Critical values for a steady-state identifier. *J. Process Control,* **7,** 149-152.

Charbonnier, S., C. Garcia-Beltan, C. Cadet and S. Gentil (2005). Trends extraction and analysis for complex system monitoring and decision support. *Eng. Appl. Artif. Intell.,* **18,** 21-36.

Cheung, J.T.Y. and G. Stephanopoulos (1990). Representation of process trends - part I. a formal representation framework. *Comput. Chem. Eng.,* **14,** 495-510.

Dash, S., M.R. Maurya and V. Venkatasubramanian (2004). A novel interval-halving framework for automated identification of process trends. *AIChE J.,* **50,** 149-162.

American Public Health Association (APHA), American Water Works Association (AWWA) & Water Environment Federation (WEF) (2005). *Standard Methods for the Examination of Water & Wastewater: Centennial Edition* (Eaton, A.D., L.S., Clesceri, E.W., Rice, A.E., Greenberg, M.A.H. Franson, (Eds.)), Washington D.C., 1368 pp.

Flehmig, F., R.V. Watzdorf and W. Marquardt (1998). Identification of trends in process measurements using the wavelet transform. *Comput. Chem. Eng.,* **22,** S491-S496.

Ganesan, R., T.K. Das and V. Venkataraman (2004). Wavelet-based multiscale statistical process monitoring: A literature review. *IIE Trans.,* **36,** 787-806.

Keser, B. (2008). Integration of a phosphate analyzer in a pro-active maintenance concept for water quality monitoring. Diplomarbeit, Universität Duisburg-Essen/Université Laval, 67pp.

Olsson, G., Nielsen, M., Yuan, Z., Lynggaard-Jensen, A., Steyer, J.-P. (2005). *Instrumentation, Control and Automation in Wastewater Systems.* IWA Scientific & Technical Report No. 15. IWA publishing, London, 264 pp.

Rengaswamy, R. and V. Venkatasubramanian (1995). A syntactic pattern-recognition approach for process monitoring and fault diagnosis. *Eng. Appl. Artif. Intell.,* **8,** 35-51.

Rieger, L. and P.A. Vanrolleghem (2008). mon*EAU*: a platform for water quality monitoring networks. *Wat. Sci. Technol.,* **57**(7), 1079-1086.

Rosén, C., J. Röttorp and U. Jeppsson (2003). Multivariate monitoring: challenges and solutions for modern wastewater treatment operation. *Wat. Sci. Technol.*, 47(2), 171-179.

Rubio, M., Colomer J, M. L. Ruiz, Colprim J and J. Mélendez (2004). Qualitative trends for situations assessment in SBR wastewater treatment process. In: *Proceedings of the 4th ECAI Workshop on Binding Environmental Sciences and Artificial Intelligence (BESAI)*, August 2004, Valencia, Spain.

Stephanopoulos, G., G. Locher, M. J. Duff, R. Kamimura and G. Stephanopoulos (1997). Fermentation database mining by pattern recognition. *Biotechnol. Bioeng.,* **53,** 443-452.

Thomann, M., Rieger, L., Frommhold, S., Siegrist, H. and Gujer, W. (2002). An efficient monitoring concept with control charts for on-line sensors. *Wat. Sci. Technol*. **46**(4-5), 107-116.

Villez, K. (2007). Multivariate and qualitative data analysis for monitoring, diagnosis and control of sequencing batch reactors for wastewater treatment. Ph.D. thesis, Ghent University, Gent, Belgium.

Villez, K., C. Rosén, F. Anctil, C. Duchesne and P.A. Vanrolleghem (2008). Qualitative representation of trends: an alternative approach to process diagnosis and control. *Wat. Sci. Technol.,* **57**(10), 1525–1532.

Villez, K., C. Rosén, F. Anctil, C. Duchesne and P.A. Vanrolleghem (submitted). Qualitative representation of trends: an improved method for multiscale extraction of trends from process data. Submitted to *Comput. Chem. Eng.*

Wang, X.Z. and R.F. Li (1999). Combining conceptual clustering and principal component analysis for state space based process monitoring. *Ind. Eng. Chem. Res.,* **38,** 4345-4358.